American Journal of Science and Technology
2015; 2(2): 55-73
Published online March 10, 2015 (http://www.aascit.org/journal/ajst)
ISSN: 2375-3846

Keywords
Tundish Flow,
Two-Fluid Model of Turbulence,
Intermittency Factor,
Two Scale k-ε Turbulence Model,
Real Power Law Fluid,
Isothermal Condition,
Non Isothermal Condition

Received: February 1, 2015
Revised: February 16, 2015
Accepted: February 17, 2015

Tundish Operation of a Two Fluid Model Using Two Scale k-ε Turbulence Model in a Real Power Law Fluid

S. Anestis

Department of Oenology and Beverage Technology, Technological Educational Institute of Athens, Faculty of Food and Nutrition, Greece

Email address
Anestis@essolutions.eu

Citation
S. Anestis. Tundish Operation of a Two Fluid Model Using Two Scale k-ε Turbulence Model in a Real Power Law Fluid. *American Journal of Science and Technology.* Vol. 2, No. 2, 2015, pp. 55-73.

Abstract
A two-fluid model of turbulence is presented and applied to flow in tundishes. The original fluid is modelled as a real power-law fluid, where we define the coefficients k and n of it. The problem was solved for isothermal and non-isothermal conditions of continuous casting (CC) tundish. Transport equations are solved for the variables of each fluid, and empirical relations from prior works are used to compare the model results. For the calculated real fluid, we compare the classic k-ε turbulence model and the new promised two scale k-ε turbulence model in isothermal and non-isothermal conditions. We optimize our results by presenting a new estimation in mass transfer rate calculation and in the intermittency factor, which the last provides a measure of the extent of turbulence in the tundish. Finally, we defined then two-fluid empirical coefficients c_f, c_h, c_m for a real non-isothermal fluid.

1. Problem Considered

Tundishes have been well studied and it is readily accepted that tundish phenomena may play a critical role in affecting steel quality. For this reason, a detailed examination of tundish problems may be an excellent illustration of the potential uses of the two fluid models in metallurgical practice.

Let us consider an industrial scale tundish system, such as shown in Schema. 1, having a single inlet and a single outlet and containing no dams or weirs. Such tundishes do exist in practice and should represent the extreme cases of potential flow mal distribution.

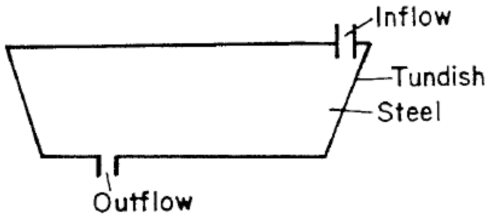

Schema 1. *Sketch of a single strand tundish*

The idea of thought of turbulence as a mixture of two liquids, each moving semi-independently in the same area, was presented by Reynolds (1874) and Prandtl (1925),

as they considered which way can the mass, momentum and energy transported in turbulence fluids. Recent proponents of this idea are the Spiegel (1972), Libby (1975), Dopazo (1977), Bray (1981), Spalding (1982) and Kollmann (1983). The above idea of separating a liquid into two sub-liquids helps us to understand more easily cases such as when the two liquids have different chemical compositions, e.g. cold unburned gas and hot combustion products.

With the above vision, each fluid is supposed to hold in any position in space and time, its own data such as speed, temperature, composition of the different variables such as volume fractions and (perhaps) and pressure. The volume fractions can be considered as "likely presence". The two liquids can be distinguished in many ways, but all of them are arbitrary. Thus, e.g. the Reynolds and Prandtl distinguish the direction of motion, such as the liquid moves to a surface that is supposed to have different properties momentum along the surface relative to the fluid moves away from it. For cases that have flows in the atmosphere, the separation of fluids is due to the upward movement of air in relation to the downward movement or the temperature of a stream that is often very different from that of another power.

The scope of this paper is to present the new two scale k – ε turbulence model and compare its result with the classical k – ε turbulence model, [Anestis, 2014]. The input parameters chosen for the purpose of the calculation are summarized in Table 1 and these are thought to be typical of the operation of tundishes employed in slab casters. Also, we suppose that our fluid is a real non Newtonian fluid (power-law) and we found its fluid coefficients k and n. The density of our fluid is calculated by Ramirez et al. (2000) equation and the mass transfer rate by Sheng and Jonsson (2000) type. Finally, we specify the empirical constants of c_f, c_h, c_m for our full case.

Table 1. *Important geometrical parameters and physical properties for the real liquid*

Parameter	Simulation value
Tundish width at the free surface [m]	2.03
Tundish width at the bottom [m]	1.20
Tundish length at the free surface [m]	9.15
Tundish length at the bottom [m]	8.50
Bath depth [m]	0.70
Distance between inlet and outlet [m]	7.48
Volumetric flow rate at inlet [lt/h]	1067
ΔT [C]	+50
Heat capacity – c_p [J/Kgr K]	750
Heat conductivity – k_o [W/mk]	41
Kinematics viscosity – ν [m^2/s]	$0.913 * 10^{-6}$
Gravity acceleration – g [m/s^2]	9.81
Thermal conductivity	$1.27 * 10^{-4}$
Density for isothermal fluid [kgr/m^3]	8523

2. Methods of Solution

As the phases completely fill the available space, the volume fractions sum to unity:

$$r_1 + r_2 = 1 \quad (1)$$

Where r_1 is the volume fraction of the first liquid that is characterized as a carrier (carrier) and r_2 is the volume fraction of the second liquid characterized as dispersed (dispersed). Thus, at any position within the container our two average flow quantities like whichever speed, temperature and concentration. In case one of the two phases volume fractions, r_1, r_2 take the value 1, then the equation (1) will give us solutions for single phase fluid.

The prediction of multiphase phenomena involves computation of the values of up to 3 velocity components for each phase, u_i and 1 volume fraction for each phase, r_i and possibly for temperature, chemical composition, particle size, turbulence quantities, pressure for each phase. Specific features of the solution procedure are, [Anestis, 2014]:

- Eulerian-Eulerian techniques using a fixed grid, and employing the concept of 'interpenetrating continua' to solve a complete set of equations for each phase present;
- The volume fraction, R_i, of phase is computed as the proportion of volumetric space occupied by a phase;
- It can also be interpreted as the probability of finding phase i at the point and instant in question;
- All volume fractions must sum to unity;
- Each phase is regarded as having it's own distinct velocity components.
- Phase velocities are linked by interphase momentum transfer - droplet drag, film surface friction etc.
- Each phase may have its own temperature, enthalpy, and mass fraction of chemical species.
- Phase temperatures are linked by interphase heat transfer.
- Phase concentrations are linked by interphase mass transfer.
- Each phase can be characterized by a 'fragment size'. This could be a droplet or bubble diameter, film thickness or volume/surface area.
- Phase 'fragment sizes' are influenced by mass transfer, coalescence, disruption, stretching etc.
- Each phase may have its own pressure - surface tension raises the pressure inside bubbles, and interparticle forces prevent tight packing, by raising pressure.
- The equations describing the state of a phase are basically the Navier-Stokes Equations, generalized to allow for the facts that:
- Each of the phases occupies only a part of the space, given by the volume fraction; and
- The phases are exchanging mass and all other properties.
- The task is to provide equations, from the solution of which values of r_i, u_i, v_i, w_i, T_i, C_i, and so on can be deduced.
- The mathematical model is based on solving equations of the 3D Navier-Stokes. Speeds, temperatures, and the volume fractions provided for both liquids over the whole field, based on the visa of Euler.

- The two liquids share the same pressure and the distribution of turbulence disturbance inside the area, because both of them, where the continuous phase and the physical properties are similar. Thus, the pressure P is common to both phases.
- The calculations are performed assuming that we are in full state (steady state), and the field calculation can be simplified because of the symmetric geometry.
- The standard k-ε turbulence model with the two equations used to describe the turbulence of the two liquids within the sector.
- The top surface of the tundish was taken to be a free surface where a zero shear stress condition was applied according to references, [Illegbussi et al., 1991 and 1992].
- The free surface was considered to be flat.
- For the free surface and symmetry plane, the normal gradients of all variables were set to be zero.
- The heat exchange between the liquid metal and the air can be ignored. This could be justified because of the small temperature difference and the short period of modeling.
- Each phase can have its own unique speed, temperature, enthalpy, and the mass fraction of chemical species.
- The temperatures of each phase associated with the transfer of heat to the common boundary (interphase).
- The concentrations of each phase associated with the mass transfer in one limit (interphase).
- Each phase can be characterized by a "fragment size". This could be a drop or bubble diameter, thickness, or volume / surface. The 'fragment sizes' affected by mass transfer, the combination, inconvenience, etc.
- The equations that describe the state of the phase are generalized equations Navier-Stokes. Each one of the phases only occupies a portion of space, given by the volume fraction. The phases exchange of mass and all other properties. The objective is to solve the equations and the determination of r_i, u_i, v_i, w_i, T_i, C_i [Anestis, 2014B].

3. The Generalizing Equations

The model assumes that the system consists of two fluids. The inlet stream, with the temperature variation, is considered as the first fluid. The original liquid in the tundish is considered as the second fluid. The two-fluids assumed to share space in proportion to their volume fractions so as to satisfy the following total continuity eq.1:

In case that we have a three dimensional, steady, non-isothermal, one phase, two-fluid and turbulence fluid flow in tundish, we can write the general equation as follows:

$$\frac{\vartheta}{\vartheta t}(r_i\rho_i\Phi_i) + \frac{\vartheta}{\vartheta x_j}\left(r_i\rho_i u_j\Phi_i - r_i\Gamma_{\Phi i}\frac{\partial\Phi_i}{\partial x_j} - \Phi_i\Gamma_{ri}\frac{\partial r_i}{\partial x_j}\right) = S \quad (2)$$

In which $\Gamma_{\varphi i}$ is within-phase diffusion coefficient [Ns/m^2], Γri is the phase coefficient [Ns/m^2], S is the total sources. We must notice that the $\Gamma_{\varphi i}$ within-phase diffusion coefficient represents the molecular and turbulence mixing present in the phase. The Γ_{ri} the phase coefficient represents the transport of Φ brought by the turbulence dispersion of the phase itself. The next Table 2 defines the above coefficients. Many times we represent the eq.2 with the next form which is equivalent.

We must notice that in eq.2 the first term presents the transient quantities, the second the convection quantities, the third the within-phase diffusion quantities, the fourth the without-phase diffusion quantities and the fifth the interphase volumetric sources.

$$\frac{\vartheta}{\vartheta t}(r_i\rho_i\Phi_i) = \text{transient sources}$$

$$\frac{\vartheta}{\vartheta x_j}\left(r_i\rho_i u_j\Phi_i\right) = \text{convection sources}$$

$$\frac{\vartheta}{\vartheta x_j}\left(r_i\Gamma_{\Phi i}\frac{\partial\Phi_i}{\partial x_j}\right) = \text{within phase diffusion sources}$$

$$\frac{\vartheta}{\vartheta x_j}\left(\Phi_i\Gamma_{ri}\frac{\partial r_i}{\partial x_j}\right) = \text{phase diffusion sources}$$

The transient, convective and diffusion terms contain the appropriate volume fraction multiplier or upwind or averaged. Also, the links between the phases (mass, momentum and heat transfer) are introduced via an interphase source.

Table 2. *Diffusion flux coefficients and source terms for the two-fluid model.*

Equation	Φ	$\Gamma_{\varphi i}$	S	
			$S_{\varphi i}^{ii}$	$S_{\varphi i}^{ij}$
Continuity	1	0	0	E_{ij}
Momentum	u,v,w	$c_t l r_i r_j \lvert\Delta u\rvert$	$-r_i\nabla p + F_b + G_{sh}$	$F_{ij} + U_j E_{ij}$
Energy	C_p*T_i	$c_t l r_i r_j \lvert\Delta u\rvert\sigma_t$	0	$Q_{ij} + c_p T_j E_{ij}$
Temperature	T	$\frac{\mu_l}{\sigma_l} + \frac{\mu_t}{\sigma_t}$		

The quantities in the table 2 analyzied as:

$$G_{sh} = c_v r_i \lvert\Delta U\rvert\lvert\frac{\partial w}{\partial y}\rvert \quad (3)$$

$$E_{ij} = c_m \rho_i l^{-1} r_i r_j \lvert\Delta u\rvert \quad (4)$$

$$F_{ij} = c_f \rho l^{-1} r_i r_j (U_i - U_j)\lvert\Delta u\rvert = \frac{c_f}{c_m} E_{ij}(U_i - U_j) \quad (5)$$

$$Q_{ij} = c_h c_p \rho_i l^{-1} r_i r_j (T_i - T_j)\lvert\Delta u\rvert = \frac{c_h}{c_m} E_{ij}(U_i - U_j) \quad (6)$$

$$\Gamma_{\varphi i} = \rho_i\left(\frac{\nu_{li}}{Pr_{li}} + \frac{\nu_{ti}}{Pr_{ti}}\right) \quad (7)$$

$$\Gamma_{ri} = \rho_i\left(\frac{\nu_{li}}{Pr_{li}} + \frac{\nu_{ti}}{Pr_{ti}}\right)\frac{\theta r_i}{\theta x_i} \quad (8)$$

- μ_{eff} is the effective viscosity which is the sum of the molecular and the turbulence contributions. The turbulence viscosity μ_t is strongly position dependent and is a function of the velocity gradients prevailing at the particular location. Using the Kolmogorov – Prandtl model for the turbulence effective viscosity, we take the form:

$$\mu_t = c_\mu \rho \frac{k^2}{\varepsilon} = c_\mu \rho \varepsilon^{1/2}\lambda_\mu \quad (9)$$

Where ε is the turbulence energy and λ_μ is the length scale of viscosity from van Driet's proposoal in the following form:

$$\lambda_\mu = d(1 - e^{-A_\mu Re_t}) \quad (10)$$

$$Re_t = \frac{d\rho\varepsilon^{1/2}}{\mu} \quad (11)$$

Here, D is the shortest distance to the solid boundaries, Re_t is the turbulence Reynolds number in that point, and A_μ is an empirical coefficient.

- G_{sh} appears only in the cross stream momentum equation,
- $E_{ij}$is the model for the volumetric entrainment of non turbulence fluid
- $F_{ij}$is the inter fluid function friction forces.
- $Q_{ij}$is the conductive heat transfer across the turbulence – non turbulence interface.
- $S_{\varphi i}^{ii}$is an intra-fluid source term such as that resulting from pressure gradients, body forces, velocity gradients, etc
- $S_{\varphi i}^{ij}$ is an inter-fluid source term due to entrainment of one fluid by the other, friction and heat conduction at the interface
- The term |ΔU| is the characteristic "slip velocity" with which the individual fluid momentum and temperatures are transported to the interface.
- Also, (U_j-U_i) express the local fluctuations in velocity and (T_j-T_i) the local fluctuation in temperature.
- The c_p, σ_{kp}, $\sigma_{\varepsilon p}$, c_{p1}, c_{p2}, c_{p3}, c_μ, σ_{KT}, σ_ε, c_{T1}, c_{T2} and c_{T3} are empirical constants which have been calculated by others, Table 3.
- The rations c_f/c_m and c_h/c_m are characteristic quantities of the flow and must be calculated here.
- F_b is the body force while G_{sh} is a source term due to velocity gradients which accounts for tendency of a shear layer to break up into a succession of eddies. This term is negligible for the main stream momentum equation, but takes the following form for the cross stream momentum equation, when w is the mean stream-wise velocity.
- Also F_{ri} is the phase diffusion coefficient in Ns/m^2 and $F_{\varphi i}$ is the within-phase diffusion coefficient in Ns/m^2.
- The effective thermal conductivity, k_{eff}, consists now of two components, where Pr_t is the turbulence empirical Prandtl number and is equal to 0.9

Since, it is known that turbulence can disappear completely, the assumption that turbulence fluid cannot enter the non-turbulence area, is at variance with the facts. This defect may be as serious as is sounds in most cases.

Table 3. *Empirical constants in the computation*

C_v	C_t	P_{rt}	C_m	C_d	C_f	C_h
0.30	10.0	0.90	10.0	1.0	0.05	0.05
σ_t	c_1	c_2	c_μ	σ_k	σ_e	
1.0	1.44	1.92	0.09	1.0	1.3	

- The non-dimensional drag coefficient c_d is a function of the bubble Reynolds number, defined as Re_{bub}

$$Re_{bub} = \frac{\rho_l|v_l - v_g|D}{\mu_t} \quad (12)$$

The function $c_d(Re_{bub})$ may be determined experimentally, and is known as the drag curve. The drag curve for bubbles can be correlated in several distinct regions:

1) Stokes regime,

$$0 \le Re_{bub} \le 0.2,\ c_d = \frac{24}{Re_{bub}} \quad (13)$$

2) Allen regime,

$$0 \le Re_{bub} \le 500\sim1000,\ c_d = \frac{24}{Re_{bub}}(1 + 0.15Re_{bub}^{0.687}) \quad (14)$$

3) Newton regime,

$$500\sim1000 \le Re_{bub} \le 1\sim2 * 10^5,\ c_d = 0.44 \quad (15)$$

4) Super critical regime

$$Re_{bub} \ge 1\sim2 * 10^5\ c_d = 0.1 \quad (16)$$

Analysis of the results revealed that most bubbles are in the Allen regime area. In case that we have one fluid, then replacing the r_1=r_2=1 we take the next Table 4 with the analogous generalized equation:

Table 4. *Diffusion flux coefficients and source terms for the one-fluid model.*

Equation	Φ	Γ	S
Conservation of Mass	1	0	0
Momentum	u,v,w	μ_{eff}	$\frac{\theta}{\theta x_j}(\mu_{eff}\frac{\theta u_j}{\theta x_j})$
Kinetic Energy	K	$\frac{\mu_{eff}}{\sigma_K}$	G - ρεc_d
Dissipation rate	ε	$\frac{\mu_{eff}}{\sigma_\varepsilon}$	$\frac{g}{K}(C_1G - C_2\rho\varepsilon)$
Enthalpy	T*c_p	k_{eff}	0

The quantities in the table 4 analyzied as:

$$\mu_t = \frac{\rho C_d k^2}{\varepsilon} \quad (17)$$

$$\mu_{eff} = \mu_t + \mu_l \quad (18)$$

$$\nu_t = c_\mu f_\mu \frac{k^2}{\varepsilon} = f_\mu \frac{\mu_t}{\rho} \quad (29)$$

$$k_{eff} = k_0 + c_p \frac{\mu_t}{Pr_t} \quad (20)$$

$$G_k = \mu_t \frac{\partial u_j}{\partial x_i}\left(\frac{\partial u_i}{\partial x_j} + \frac{\partial u_j}{\partial x_i}\right) \quad (21)$$

4. Continuity Equations

The way to calculate the mass transfer rate between the two fluids there are two popular equations. The first equation is [Yu et al., 2007; Malin and Spalding, 1984; Shen et al., 2003; Markatos et al., 1986; Ilegbussi, 1994; Markatos and Kotsifaki, 1994]:

$$\dot{m} = c_m \rho_1 l^{-1} r_1 r_2 |\Delta U| \quad (22)$$

And the second one is [Sheng and Jonsson, 2000]:

$$\dot{m} = c_m \rho_1 l^{-1} r_1 r_2 (r_2 - 0.5) |\Delta U| \quad (23)$$

In the above equations, r_i is the phase volume fraction [m^3/m^3], ρ_i is the phase density, [kg/m^3], u_i is the phase velocity vector [m/s] and m_{ji} is the net rate of mass entering phase i from phase j [$kg/(m^3 s)$]. The mass transfer rate equation between the two fluids plays a very important role in the two-fluid model. Eqs.22 and 23 are the most widely used relations. In eq.22 m is always positive, which means that only fluid 2 (non – turbulence fluid) can be entrained by fluid 1 (turbulence fluid). According to eq.23 the m may be been negative. The additional factor ($r_2 - 0.5$) allows for the equally entrainment between the turbulence fluid 1 and the non-turbulence fluid 2. From the view point of physics, the entrainment rate of anon turbulence fluid by a turbulence fluid is much more than that of the turbulence fluid by the non-turbulence fluid. So, eqs.22 and 23 have disadvantages and a new more aqua rate mass transfer rate equation should be developed. Here, we used the eq.23. Finally, there is no the phase of diffusion term J_{ri}, which models the turbulence dispersion of particles by random motion mechanism. It is not present in laminar flows.

5. Density Relationships

Consequently, a non-isothermal situation exists in the tundish and the flow patterns in such cases may be quite different from those obtained under isothermal conditions. For non-isothermal conditions many writers expressed the relationship between the density and the temperature of the water with many different equations. For the case that we want to have real steel, the most common used expression, which we will be used in this thesis is, [Joo et al.,1993; Ramirez et al., 2000]:

$$\rho = 8523 - 0{,}8358 * T \quad (24)$$

In order to take into consideration thermal natural convection phenomena, a set of typical boundary conditions was chosen. These included steady-state flows and heat losses and an overlaying slag wetting to inclusions.

6. Boundary Conditions

The flow in a tundish is from the top left hand corner. The flow field is computed by solving the mass and momentum conservation equations in a boundary fitted coordinate system along with a set of realistic boundary conditions. The tundish boundary conforms to a regular Cartesian system. The free surface of the liquid in the tundish was considered to be flat and the slag depth was considered to be insignificant. With these two assumptions the flow field was solved with the help of the above equations for all the cases. The effect of natural convection is ignored in the tundish because the ratio, $Gr/Re^2 = 0.044\Delta T$ [Lopez-Ramirez et al., 2000], where ΔT, the driving force for natural convection, is the temperature difference between the liquid steel at the top free surface of the tundish and the bulk temperature of the liquid, is much less than unity for all the cases that are computed here.

The formation of waves at the free surface was ignored. The free surface was assumed to be flat and mobile. Fluxes of all quantities across the free surface were assumed to be zero [Szekely et al., 1987; Tacke et al., 1987; Ilegbussi et al., 1988]. Therefore, normal velocity component (for convective flux) and normal gradients of all variables (for diffusive flux) were all set to zero, i.e.

$$w = 0, \frac{\partial u}{\partial z} = 0, \frac{\partial v}{\partial z} = 0, \frac{\partial k}{\partial z} = 0, \frac{\partial \varepsilon}{\partial z} = 0 \quad (25)$$

The tundish exit can be computationally treated as either a standard outflow or as a plane or surface, at which flow occurs at an ambient pressure (taken). At the tundish outlets, both types of boundary conditions were applied in order to assess the similarity of the experimental results to model configuration. At all the solid walls, the velocity components was set to zero, at both the side walls, at both the frontal side walls and at the bottom wall:

$$u=0,\ v=0,\ w=0,\ k=0,\ \varepsilon=0 \quad (26)$$

Finally, the wall of the tundish was considered to be impervious to the dye, so a zero gradient condition for the dye was used on the walls. At the outlet and the inlet at the free surface also zero gradient conditions were used for the dye [Ilegbussi et al. 1988 and 1989].

7. Near Wall Nodes

The viscous sub-layer is bridged by employing empirical formulas to provide near-wall boundary conditions for the mean flow and turbulence transport equations. These formulae connect the wall conditions (e.g. the wall shear stress) to the dependent variables at the near-wall grid node which is presumed to lie in fully-turbulence fluid. Strictly, wall functions should be applied to a point whose Y^+ value is in the range $30 < Y^+ < 130$, where u_T is the friction velocity

$$y^+ = \frac{u_T}{\nu_l} y \quad (27)$$

$$u_T = \sqrt{\frac{\tau_w}{\rho}} \quad (28)$$

The advantages of this approach are that it escapes the need to extend the computations right to the wall, and it avoids the need to account for viscous effects in the turbulence model. The log-law is extended to non-equilibrium conditions, as follows:

$$\frac{U\sqrt{k}}{u_T} = \frac{ln\left(\frac{E_{st}\sqrt{k}}{\nu_l} y\right)}{K_{st}} \quad (29)$$

$$K_{st} = k\left(c_\mu c_d\right)^{1/4} \quad (30)$$

$$E_{st} = E\left(c_\mu c_d\right)^{1/4}. \quad (31)$$

The turbulence friction factor s_{turb} and Stanton number St_{turb} are now given by:

$$S_{turb} = \frac{K_{st}\sqrt{KE}}{U_r ln\left[E_{st}\sqrt{KE}\frac{Y}{ENUL}\right]} \quad (32)$$

$$St_{turb} = \frac{S_{turb}}{P_{rT}\left[1+\frac{P_m S_{turb} U_r}{\left(c_\mu c_d\right)^{1/4}\sqrt{KE}}\right]} \quad (33)$$

The value of k at the near-wall point is calculated from its own transport equation with the diffusion of energy to the wall being set equal to zero. The mean values of P_k and ε over the near-wall cell are represented in the transport equation for k as:

$$P_k = \frac{U_s^2 U_r}{2Y} \quad (34)$$

$$\varepsilon = (c_\mu c_d)^{3/4} k^{3/2} \frac{ln\left(E_{st}\sqrt{k}\frac{y}{\nu_l}\right)}{2ky} \quad (35)$$

However, in the formula for the near-wall eddy viscosity, ε is calculated from

$$\varepsilon = (c_\mu c_d)^{3/4} \frac{k^{3/2}}{2ky} \quad (36)$$

The non-equilibrium wall functions will give better predictions of heat transfer coefficients at a reattachment point. Attention is restricted to boundary conditions for the k-ε model.

- The normal gradients are zero for both K and ε.
- In many cases, a free surface can be considered to a first approximation as a symmetry plane.
- A fixed-pressure condition is employed at free boundaries, which involves prescribing free stream values for K and ε. If the ambient stream is assumed to be free of turbulence, then K and ε can be set to negligibly small values.
- The inlet values of K and ε are often unknown, and the advice is to take guidance from experimental data for similar flows. The simplest practice is to assume uniform values of K and ε computed from:

$$k_{in} = (Iu)^2 \cong 0.01 u_{in}^2 \quad (37)$$

$$\varepsilon_{in} = \left(c_\mu c_d\right)^{3/4} \frac{k^{3/2}}{LM} \cong \left(c_\mu c_d\right)^{3/4} \frac{k^{3/2}}{R} \quad (38)$$

$$I = \sqrt{\frac{W^2}{W_{inlet}}} \quad (39)$$

Where I is the turbulence intensity (typically in the range 0.01<I<0.05) and LM~0.1H, where H is a characteristic inlet dimension, say the hydraulic radius of the inlet pipe. Many times but not often responsible for poor convergence, is the use of unrepresentative initial K and ε values which can lead to a convergence problem.

8. Estimation Factors

1. Discretization schemes are 2nd order for pressure and 2nd order upwind for all other equations.
2. The convergence criterion for scaled residuals was set to be less than 10^{-3}.
3. The relaxation factors are for pressure a_P=0.3, for momentum is $a_{u,v,w}$=0.7 and for turbulence kinetic energy are $a_{k\text{-}e}$=0.3
4. A criterion for convergence was set to be less than 10^{-5} on all variables and computations were carried out until the relative sum of residuals on all variables all fell below the stipulated value.
5. The whole volume filled with molten steel in the tundish was chosen as the numerical calculation domain.
6. A constant mass flow rate of steel from the ladle to the tundish was used for the mathematical simulation.
7. Discretization equations were derived from the governing equations and were solved by using an implicit finite difference procedure called SIMPLE algorithmic.

9. Non-Newtonian Fluids

There are two representative options for the simulation of inelastic time-independent non-Newtonian fluids, namely the Power-law and Bingham models. The power-law model is also known as the Ostwald-de Waele model. Pseudo plastic and dilatant fluids are described by the power-law model. The former are fluids for which the rate of increase in shear stresses with velocity gradient decreases with increasing velocity gradient. Dilatant fluids are those for which the rate of increase in shear stress with velocity gradient increases as the velocity gradient is increased, [Skelland, 1967]. Many purely viscous fluids encountered in processing operations and thermal processing of liquid foods, polymers, etc. conforms to the power-law model within engineering accuracy. Other examples of power-law fluids include rubber solutions, adhesives, polymer solutions or melts, and biological fluids. A Bingham fluid is a fluid for which the imposed stress must exceed a critical yield stress to initiate motion. Examples of fluids which behave as, or nearly as, Bingham plastics include water suspensions of clay, sewage sludge, some emulsions and thickened hydrocarbon greases, and slurries of uranium oxide in nuclear reactors.

For the Power-law incompressible Newtonian fluids, the relationship between the shear stress and the shear rate may be written as:

$$\tau_{ij} = \mu \Delta_{ij} \quad (40)$$

Where τ_{ij} is the stress tensor, Δ_{ij} is the symmetrical rate-of-deformation tensor, and μ is the coefficient of apparent dynamic viscosity. For Newtonian fluids, μ depends on local pressure and temperature but not on τ_{ij} or Δ_{ij}. For the Power-law fluids, μ is a function of Δ_{ij} and/or τ_{ij}, as well as of temperature and pressure. For a power-law fluid, the non-Newtonian scalar kinematic viscosity ν is given by:

$$\nu = \frac{\mu}{\rho} \rightarrow \mu = \rho\nu = \frac{\tau}{\gamma} = K\gamma^{(n-1)} \quad (41)$$

$$\nu = \frac{K\gamma^{\frac{1}{2}(n-1)}}{\rho} \quad (42)$$

Where ρ is the local fluid density, τ is the shear stress, μ is the apparent dynamic viscosity,K is the fluid consistency index at a reference temperature; n is the power-law or flow behavior index; and γ is the shear rate, where denotes the double-dot scalar product of two tensors, is given by:

$$\gamma = 0.5(\Delta_{ij}\Delta_{ij}) \quad (43)$$

10. Turbulence Models

10.1. Standard k – ε Turbulence Model

This model is the most known all over the world. It was proposed by Harlow and Nakayama in 1968 and from there we can find many other similar models. Later, Launder and Spalding [1974] proposed a new k-ε model with inclusion of allowance for buoyancy effects.

The turbulence kinetic energy k is according the Table 5, the next one:

$$\frac{\partial}{\partial t}(\rho k) + \frac{\partial}{\partial x_i}\left(\rho u_i k - \frac{\mu_{eff}}{\delta_k}\frac{\partial k}{\partial x_i}\right) = G - \rho\varepsilon \quad (44)$$

Convection + (convection – diffusion) = production - dissipation

The turbulence rate of dissipation ε is according the Table 2, the next one:

$$\frac{\partial}{\partial t}(\rho\varepsilon) + \frac{\partial}{\partial x_i}\left(\rho u_i \varepsilon - \frac{\mu_{eff}}{\delta_\varepsilon}\frac{\partial \varepsilon}{\partial x_i}\right) = \frac{(c_1\varepsilon G - c_2\rho\varepsilon^2)}{k} \quad (45)$$

Convection + (convection – diffusion) = (total production – total dissipation)

The turbulence or eddy viscosity is computed by combining k and ε:

$$\mu_{eff} = \mu_t + \mu_l = c_\mu c_d \frac{k^{3/2}}{\varepsilon} + \mu_l \quad (46)$$

Table 5. *Variables of the k-ε turbulence model*

Equation	Φ	$\Gamma_{\varphi i}$	S	
Standard k-ε turbulence model			$S_{\varphi i}^{ii}$	
Turbulence kinetic energy in production range	k	$\mu + \frac{\nu_t}{\sigma_k}$	ρ(G-ε)	0
Dissipation rate in dissipation range	ε	$\mu + \frac{\nu_t}{\sigma_\varepsilon}$	$\rho\frac{k}{\varepsilon}(c_{e1}G - c_{e2}\varepsilon)$	0

c_1=1.44, c_2=1.92, c_μ=0.90, σ_i=1.00

The standard k-ε turbulence model is suitable for high Reynolds number. But near the walls, where the Reynolds number tends to zero, the model requires the application of the so called 'wall functions'.

10.2. Two Scale k – ε Turbulence Model

The advantage of the 2-scale K-ε model lies in its capability to model the cascade process of turbulence kinetic energy; and to resolve the details of complex turbulence flows better than the standard k-e model. The disadvantage is that it requires 4 turbulence transport equations, as opposed to the 2 equations required for the standard k-ε model, Table 6. The recommendation is that the standard k-ε model or one of its variants be used in the first instance. However, in cases where these models are clearly giving poor predictions the 2-scale model should be used to see whether better predictions can be obtained.

The dissipation rate ε in the K-ε model can be regarded as the rate at which energy is being transferred across the spectrum from large to small eddies. The standard K-ε model assumes spectral equilibrium, which implies that, once turbulence energy is generated at the low-wave-number end of the spectrum (large eddies), it is dissipated immediately at the same point at the high-wave-number end (small eddies). In general, this is not the case, because there is a vast size disparity between those eddies in which turbulence production takes place, and the eddies in which turbulence dissipation occurs. In some flows there is an appreciable time lag between the turbulence production and dissipation processes, during which time the large- scale turbulence is continually being broken down into finer and finer scales.

The Hanjalic and co-workers [1978 and 1980] proposed a two-scale model in which the turbulence- energy spectrum is divided into two parts, roughly at the wave number above which no mean-strain production occurs. The first part is termed the 'production' region and the second part the 'transfer' region. Spectral equilibrium is assumed between the transfer region and the region in which turbulence is dissipated. The total turbulence energy, k, is assumed to be divided between the production region (K_P) and the transfer region (K_T). Two transport equations are employed to describe the rate of change of turbulence energy associated with each of the two regions. The closure of these equations is accomplished by defining ε as the rate of energy transfer out of the production region, so that E_P serves as a sink in K_P and as a source of K_T, while the dissipation rate E_T defines the sink of K_T. The assumption of spectral equilibrium between the transfer and dissipation regions means that E_T is the dissipation rate. Hence, four turbulence parameters, K_P, K_T, E_P and E_T are used to characterize the production and dissipation processes. Successful applications of the foregoing two-scale simplified split- spectrum model have been reported by [Hanjalic et al,.;1978 and 1980], Fabris et al.,1981; Chen,1986]. A generalization of the model for a multiple split-spectrum case has been reported by Schiestel [1983 and 1987].

Table 6. *Variables of the 2 scale k-ε turbulence model*

Two scale k-ε turbulence model			$S_{\varphi i}^{ij}$	$S_{\varphi i}^{ii}$
Turbulence kinetic energy in production range	k_p	$\nu+\frac{\nu_t}{\sigma_{kp}}$	$\rho(G-\varepsilon_p)$	0
Turbulence kinetic energy in dissipation range	k_T	$\nu+\frac{\nu_t}{\sigma_{kT}}$	$\rho(\varepsilon_p-\varepsilon)$	0
Transfer rate in production range	ε_P	$\nu+\frac{\nu_t}{\sigma_{\varepsilon P}}$	$\rho(c_{p1}G\frac{G}{K_P}+c_{p2}G\frac{G\varepsilon_P}{K_P}-c_{p3}\varepsilon_P\frac{\varepsilon_P}{K_P}$	0
Dissipation rate in dissipation range	ε	$\nu+\frac{\nu_t}{\sigma_\varepsilon}$	$\rho(c_{T1}\varepsilon_P\frac{\varepsilon_P}{K_T}+c_{T2}\varepsilon_P\frac{\varepsilon}{K_T}-c_{T3}\varepsilon\frac{\varepsilon}{K_T}$	0
C_μ=0.5478, c_d=0.1643, δ_k=1.0, δ_ε=1.314, c_1=1.0, c_2=1.92, c_3=1.44				

The two-scale K-ε model provided in PHOENICS is also based on a simplified split-spectrum, but it employs the proposal of Kim and Chen in 1989, for variable partitioning of the turbulence kinetic- energy spectrum. This model is based on the work of Hanjalic et al [1978], but differs significantly from it in the details of the modeling. The main feature of this model is that it does not employ a fixed ratio of K_P/K_T to partition the turbulence kinetic-energy spectrum; instead, variable partitioning is used in such a way that the partition is moved towards the high-wave-number end when production is high and towards the low-wave-number end when production vanishes. The location of the partition (the ratio K_P/K_T) is determined as a part of the solution, and the method causes the effective eddy viscosity coefficient to decrease when production is high and to increase when production vanishes. The advantage of the two-scale K-ε model lies in its capability to model the cascade process of turbulence kinetic energy and its capability to resolve the details of complex turbulence flows (such as separating and reattaching flows) better than the standard K-ε model [Kim and Chen, 1989; Kim, 1990, Kim, 1991]. In this model the total turbulence energy, K_E, is divided equally between the production range and transfer range, thus K_E is given by

$$K_E = K_P + K_T$$

Where K_P is the turbulence kinetic energy of eddies in the production range and K_T is the energy of eddies in the dissipation range. For high turbulence Reynolds numbers, the total turbulence kinetic energy is $\mu_{eff} = \mu_t + \mu_l = c_\mu c_d \frac{k^{3/2}}{\varepsilon} + \mu_l$. In case that r_i = 1, the eq.1 or eq.2 with the Table 3, will take the next generalization form as:

$$\frac{\vartheta}{\vartheta t}(\rho_i\Phi_i)+\frac{\vartheta}{\vartheta x_j}(\rho_i u_j\Phi_i)=\frac{\vartheta}{\vartheta x_j}\left(\Gamma_{\Phi i}\frac{\partial\Phi_i}{\partial x_j}\right)+S_{\varphi i} \quad (47)$$

$$\frac{\vartheta}{\vartheta t}(\rho_i\Phi_i)+\frac{\vartheta}{\vartheta x_j}\left(\rho_i u_j\Phi_i-\Gamma_{\Phi i}\frac{\partial\Phi_i}{\partial x_j}\right)=S_{\varphi i} \quad (48)$$

$$\mu_{eff}=\mu_l+\mu_t \quad (49)$$

$$\mu_T=c_\mu c_d\rho\frac{k^2}{\varepsilon}=c_\mu c_d\rho\frac{k^2}{E_T}=c_\mu c_d\rho\frac{k^2}{E_P} \quad (50)$$

Where $c_\mu c_d = (c_\mu c_d)'\frac{ET}{EP}$ and $(c_\mu c_d)' = 0.09$. The functional relationship for $c_\mu c_d$ determines the location of the partition between the P and T regions. Note that for turbulence flows in local equilibrium, $P_k=E_T$ and $\varepsilon_T=\varepsilon_P$ so that. The model constants are: $PRT(k_P)$=0.75, $PRT(\varepsilon_P)$=1.15, $PRT(k_T)$=0.75, $PRT(\varepsilon_T)$=1.15, C_{P1}=0.21, C_{P2}=1.24, C_{P3}=1.84, C_{T1}=0.29, C_{T2}=1.28 and C_{T3}=1.66. Also, G is the generation term, μ_{eff} is the effective viscosity, μ_l is the laminar viscosity and μ_t is the turbulence viscosity. The μ_t turbulence viscosity is related to the turbulence energy and dissipation of turbulence energy.

The transport equations for laminar and turbulence k are:

$$\frac{\partial}{\partial t}(\rho k_P)+\frac{\partial}{\partial x_i}\left[\rho u_i k_P-\frac{\mu_T}{Prt(k_P)}\frac{\partial k_P}{\partial x_i}\right]=\rho(P_k-\varepsilon_P) \quad (51)$$

$$\frac{\partial}{\partial t}(\rho k_T)+\frac{\partial}{\partial x_i}\left[\rho u_i k_T-\frac{\mu_T}{Prt(k_T)}\frac{\partial k_T}{\partial x_i}\right]=\rho(\varepsilon_k-\varepsilon_T) \quad (52)$$

The transport equations for laminar and turbulence ε are:

$$\frac{\partial}{\partial t}(\rho\varepsilon_P)+\frac{\partial}{\partial x_i}\left[\rho u_i\varepsilon_P-\frac{\mu_T}{Prt(\varepsilon_P)}\frac{\partial\varepsilon_P}{\partial x_i}\right]=\rho\left(c_{P1}\frac{P_k^2}{k_P}+c_{P2}\frac{P_k\varepsilon_P}{k_P}-c_{P3}\frac{\varepsilon_P^2}{k_P}\right) \quad (53)$$

$$\frac{\partial}{\partial t}(\rho\varepsilon_T)+\frac{\partial}{\partial x_i}\left[\rho u_i\varepsilon_T-\frac{\mu_T}{Prt(\varepsilon_T)}\frac{\partial\varepsilon_T}{\partial x_i}\right]=\rho\left(c_{T1}\frac{\varepsilon_P^2}{k_T}+c_{T2}\frac{\varepsilon_P X\varepsilon_T}{k_P}-c_{T3}\frac{\varepsilon_T^2}{k_T}\right) \quad (54)$$

10.3. Turbulence Model and Solid Walls

Here, we will describe the development of a particular turbulence model, that in which two differential equations are solved, the dependent variables of which are the turbulence energy k and the dissipation rate of turbulence energy ε. Emphasis is given to aspects of the model having importance for flows adjacent to solid walls. Many turbulence models have been reviewed in works like [Launder and spading, 1974] and [Markatos, 1986]. In [Jha et al., 2003] compared nine different common turbulence models in tundish applications, founding that the proposed k-ε model by [Launder and Spalding, 1974], matched well with the experimental data.

The proposed for here k-ε model, [Launder and Spalding, 1974], is applicable only in regions where the turbulence Reynolds number is high. Near the walls where the Reynolds number tends to zero, the model requires the application of the called wall function model or alternatively, the introduction of a low-Reynolds number extension. For the simulation of the turbulence flow of power-law fluids with the wall function model, the use of standard wall functions is

probably questionnaire, [Skelland, 1967], and more accurate results are likely to be obtained via the use of a low-Reynolds number turbulence model or from an enhanced wall- function treatment.

The alternative to wall functions is to use a fine grid analysis in which computations are extended through the viscosity affected sub-layer close enough to the wall to allow laminar flow boundary conditions to be applied. So, the low-Re extension of Lam and Bremhorst (LB) may be applied to the standard k-ε model. The difference from the wall function model is that the model coefficients are functions of the local turbulence Reynolds number. The disadvantage of the low-Re models is that a very fine grid is required in each near wall zone. Consequently, the computer storage and runtime requirements are much greater than those of the wall function approach. For the simulation of the turbulence flow of power-law fluids with wall functions, the use of standard wall functions in these flows is probably questionable, and more accurate results are likely to be obtained via the use of a low-Reynolds-number turbulence model or from an enhanced wall- function treatment.

For the above reasons the k-ε turbulence model that we decided to work in this thesis will be the Lam-Bremhorst k-ε model. In this model, the k-ε turbulence will be used as it described by the turbulence kinetic energy k and the dissipation rate of turbulence energy ε given by the produced equations from Table 5, but the difference will be in the specification of the eddy viscosity v_t, as:

$$\nu_t = f_\mu c_\mu \frac{k^2}{\varepsilon_P} = f_\mu c_\mu \frac{k^2}{\varepsilon} \quad (55)$$

$$f_\mu = \left(1 - exp(-0.0165R_\delta)\right)^2 \left[1 + \frac{20.5}{R_t}\right] \quad (56)$$

$$f_1 = 1 + \left(\frac{0.05}{f_\mu}\right)^3 \quad (57)$$

$$f_2 = 1 - exp(-R_t^2) \quad (58)$$

$$\mathrm{Re}_{\delta=}\sqrt{\mathrm{k}}\frac{\delta}{\nu} \quad (59)$$

$$Re_t = \frac{k^2}{\nu\varepsilon} \quad (60)$$

Where f_μ, f_1, f_2 are the damping functions, dp/dz is the function pressure gradient, f is the Fanning function and y_n is the normal distance to the wall. The k-ε turbulence model is widely used and involves significant source terms in the equations for the two turbulence properties. These source terms are linearized to aid convergence, but different linearization can be chosen to suit the circumstances prevailing in the simulation. In the above eqs 55 to 60 the factors f_μ, f_1, f_2 are used in Low-Re models to incorporate effects of molecular viscosity. Also, an additional source term may be used to incorporate viscous or non-equilibrium behavior.

Table 7. *Steel properties for all the cases*

Steel property	Value	Units
Molecular viscosity μ	0.0064	Kgr/m^3
Density ρ for isothermal fluid	8523	Kgr/m^3
Density ρfor non-isothermal fluid	$\rho = 8523 - 0{,}8358T$	
Surface tension σ	1.6	N/m
Inlet kinetic energy –k_{in}	0.012810	m^2/s^2
Inlet dissipation rateε_{in}	0.016730	m^2/s^3
Flow behavior index n of power-law - n	0,1643	
Consistency flow index of power-law	0,5478	
Turbulence model k – ε coefficients	1,0	
Von karman	0,41	
Roughness parameter E	8,60	

11. The Coefficients C_m, C_f, C_h

In order to find the coefficients of two-phase flow we will start from K_f = 0.05, K_m = 0.35, K_h = 0.1, [Markatos, 1986]. The, K_f characterizes the rate of flow to the internal geometry, K_m the mass geometry and l_d is the average size fragment obtained here equal to 0.05m. These variables ranging from 0.01 <K_f <20 and 0.1 <K_m <15, [Markatos and Kotsifaki, 1994]. Our calculations based on the premise of Ilegbusi and Spalding, (1989). To calculate the coefficients C_m, C_f, C_h we made a series of runs whereas initial values, we took the values of [Ilegbusi, 1994] where applicable C_m = 10.0, C_f = 0.050 and C_h = 0.050 and 0.01 with a step up of 10. Initially, we kept prices stable C_m = 10.0, C_f = 0.050 and looked around to find the correct value of C_h for our real fluid. We calculate the change in the average temperature of the fluid as a function of our position within the boundary layer, Figure 1. The data for Figure 1 are taken from the work of Spalding (1982), as published in the work of Ilegbusi and Spalding, (1989). The comparison was made with the data of [Spaldey, 1982] and by using the relationship:

$$\mathrm{T} = \frac{\mathrm{T1-T2}}{\Delta\mathrm{T}} \quad (61)$$

In Figure 2 we change the average temperature as a function of the depth of the points within the boundary layer. The comparison was made with data from the publication [Spalding, 1982]. Having determined the exact value of the coefficient C_h we follow a similar course to compute and other factors. After several tries we ended our prices C_m = 10.0, C_f = 0.375 and C_h = 0.250 applicable to real fluid no isothermal environment, Table 8.

Table 8. *The final coefficients values for a real two-fluid fluid.*

Real fluid		
C_m	10,0	
C_f	0,375	C_m / C_f = 26.7
C_h	0,250	C_m / C_h = 40

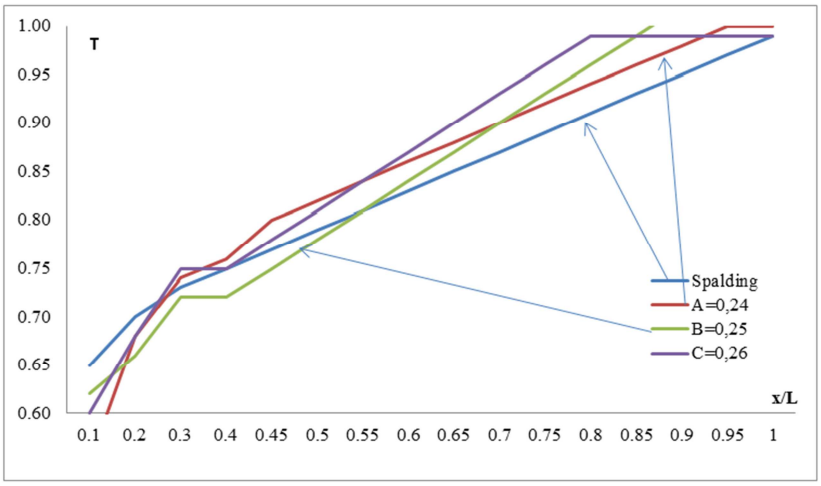

Figure 1. *The c_h according to mean differential temperature.*

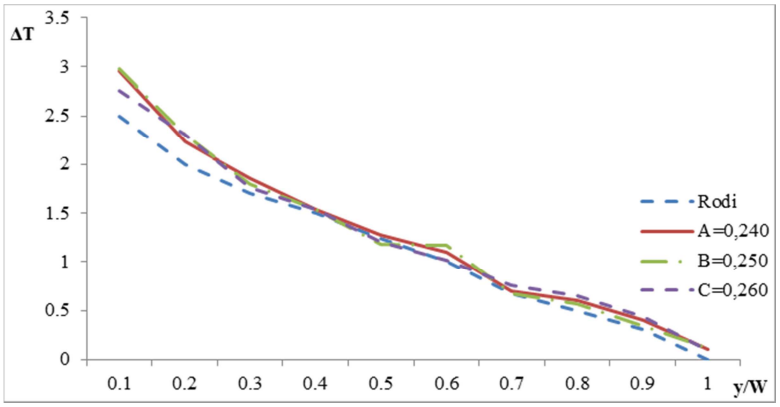

Figure 2. *The mean differential temperature values to the bounsdary layer depth.*

12. Intermittency Factor

The intermittency factor I, which has been suggested by Jones and Launder (1972) and is then explored by Libby (1975), Dopazo (1977), Byggstoyl (1981), Ilegbussi and Spalding (1987, 1989) is the percentage of the total time during which the flow are turbulence, and in the case of two-dimensional boundary layer is given by:

$$I = \min (1.0, 2r_1) \qquad (62)$$

In figure 3 we compared our intermittency factor with the experimental data of Spalding, (1983). In figure 4, we can see the change of the temperatures of the two fluids and the difference in relation to the function of depth into the boundary layer. We note initially that the difference is due to the large amount of new entry and the existing fluid. This difference disappears as we move more into our container and bring up to temperature equilibrium. The data have been compared with the publication of Leslie et al., (1970).

Finally, in figure 5 we can see the temperature profile in different places in the tundish.

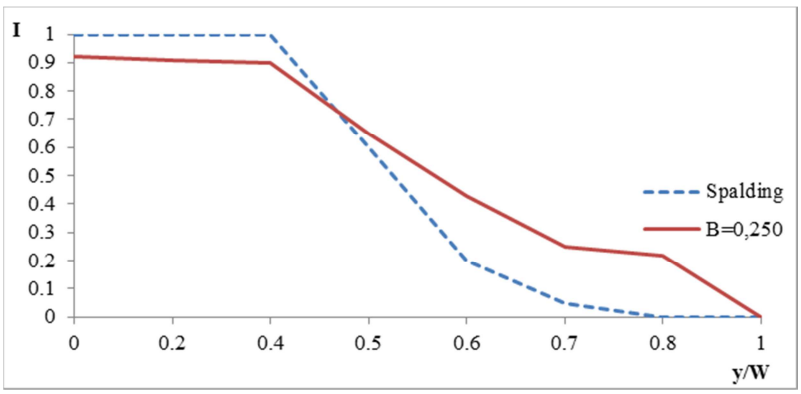

Figure 3. *The intermittency factor to mean temperature according the boundary layer depth, compare with Spalding (1983) data.*

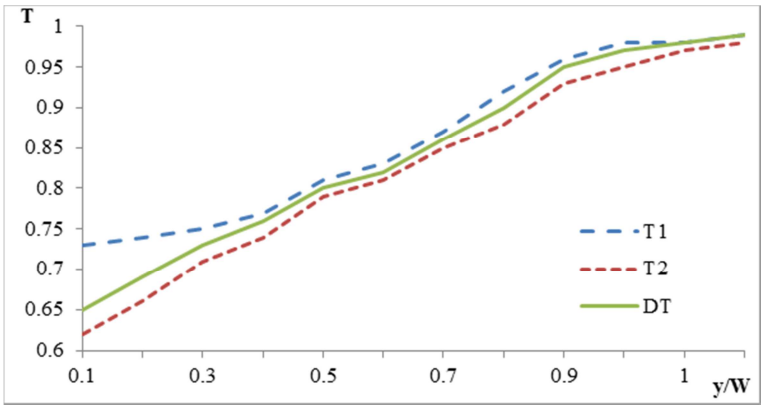

Figure 4. *The temperature to boundary layer depth.*

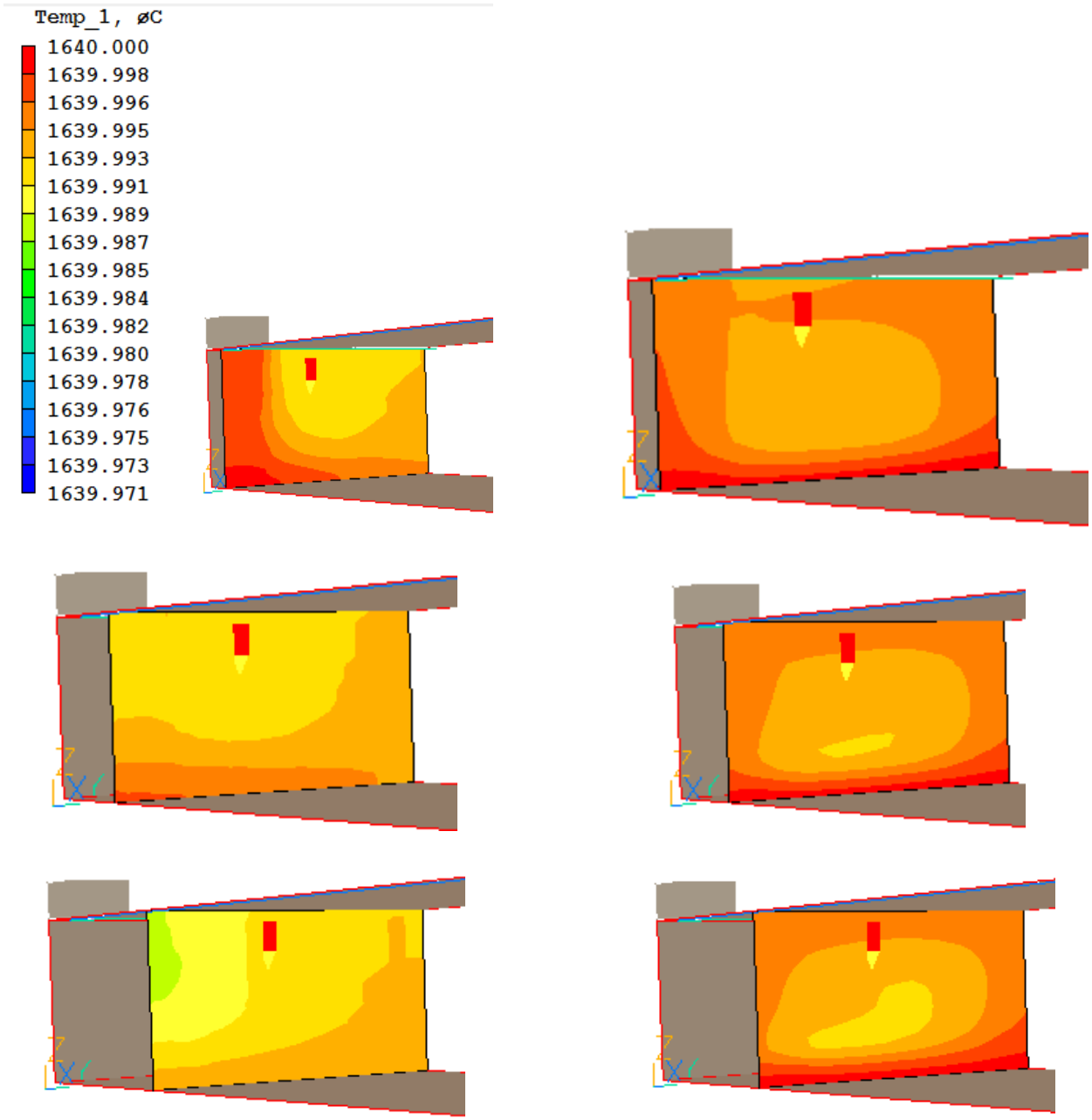

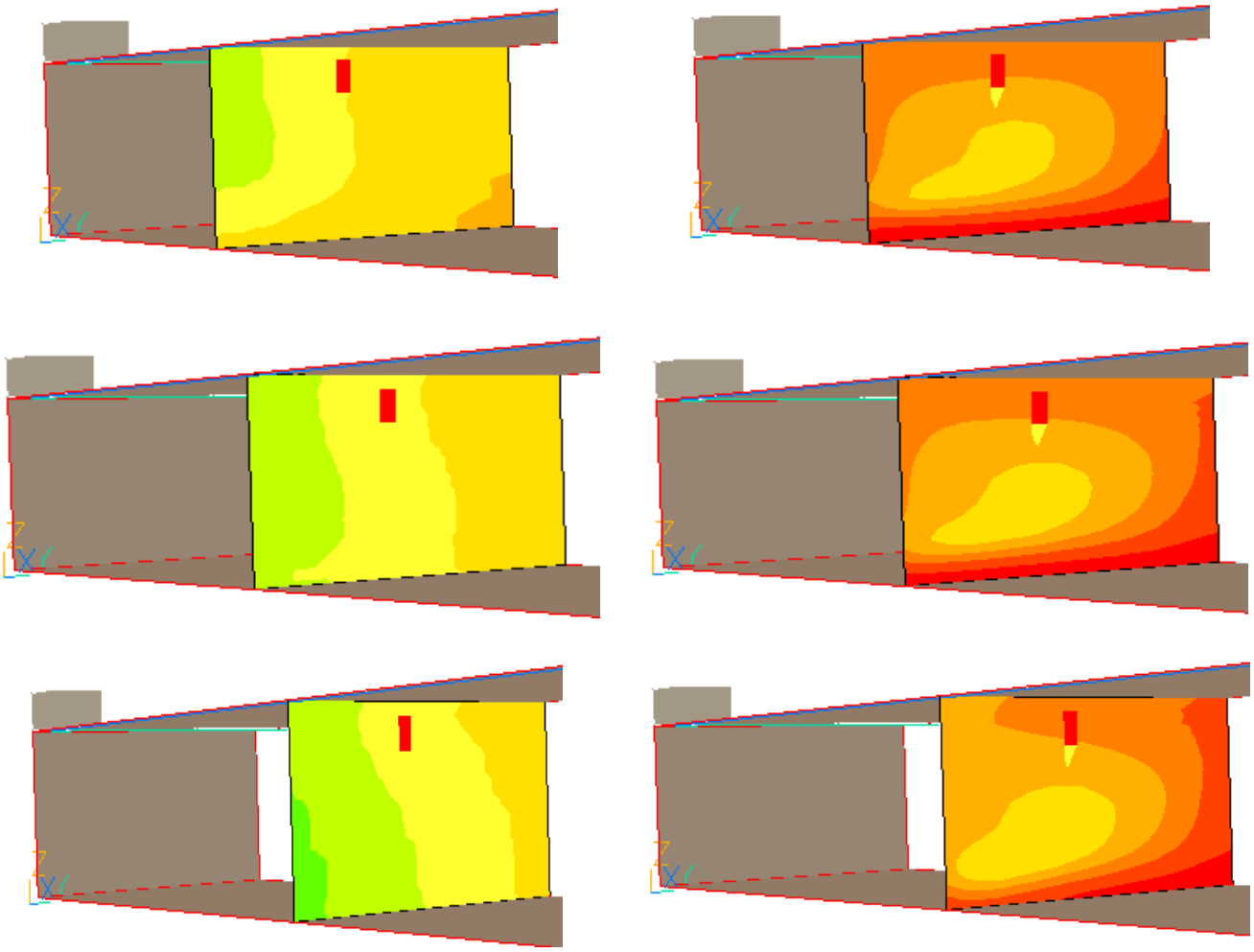

Figure 5. *The temperatures T_1 and T_2 of case P2 for different places from (0.21,0.48,0.45) to (2.65, 0.48, 0.45)*

13. The Rate of Transfer Mass

On equations of two-phase flow (cases P2 and 2P2) with symbol $\dot{m}$ we denote the rate of mass transfer between the two fluids. In literature there are two equations that estimate the above size. The first equation [Yu et al., 2007; Malin and Spalding, 1984; Shen et al., 2003; Markatos et al., 1986; Ilegbussi, 1994; Markatos and Kotsifaki, 1994] is:

$$\dot{m}_1 = c_m \rho_1 l^{-1} r_1 r_2 |\Delta U| \tag{63}$$

The second one is the Sheng and Jonsson, (2000) equation:

$$\dot{m}_2 = c_m \rho_1 l^{-1} r_1 r_2 (r_2 - 0.5) |\Delta U| \tag{64}$$

In the above equations, r_i is the phase volume fraction [m^3/m^3], P_i is the density of each phase, [kg/m^3], u_i is the velocity of each phase [m/s] and m_{ji} is the positive rate of mass entering the phase i from phase j [kg / (m^3s)]. The equation that gives the rate of mass transfer between the two fluids plays an important role in solving the equations of two-phase flow. The above equations (63) and (64) are the two most widely used. In equation (63) $\dot{m}$ size is always positive, which means that only the second liquid (the non- turbulence fluid) can be carried away from the first fluid (fluid turbulence). According to equation (64) the quantity $\dot{m}$ can be negative. The other factor (r_2 - 0.5) allows the equivalent switching between turbulence fluid 1 and 2 non- turbulence fluid. In terms of physics, the percentage of non- turbulence fluid entrained by the turbulence fluid is much more than the rate of turbulence fluid entrained by the non- turbulence fluid. Thus, equations (63) and (64) have disadvantages and for this reason should lead to a new form of the above expressions. In this paper we will use the original equation (63) and compare it with a new one that has been proposed by Yu et al. (2008) , which corresponds to the average of the two above (weight average of mass transfer rate). Yu et al. proposed the next form:

$$\dot{m}_3 = \frac{c_m \rho_1 r_1 r_2 |\Delta U|}{l} r_1 + \frac{c_m \rho_1 r_1 r_2 (r_2 - 0.5) |\Delta U|}{l} r_2 \tag{65}$$

The equations 63 and 64 can be rewritten in a new way:

$$\dot{m}_1 = c_{m1} \rho_1 l^{-1} r_1 r_2 |\Delta U| \rightarrow \frac{m_1}{\rho_1 l^{-1} |\Delta U|} = c_{m1} r_1 r_2 \tag{66}$$

$$\dot{m}_2 = c_{m2}\rho_1 l^{-1} r_1 r_2 (r_2 - 0.5)|\Delta U| \rightarrow \frac{m_2}{\rho_1 l^{-1}|\Delta U|} = c_{m2} r_1 r_2 (r_2 - 0.5) \quad (67)$$

$$\dot{m}_3 = \frac{c_{m1}\rho_1 r_1 r_2 |\Delta U|}{l} r_1 + \frac{c_{m2}\rho_1 r_1 r_2 (r_2 - 0.5)|\Delta U|}{l} r_2 \rightarrow \frac{\dot{m}_3}{\frac{\rho_1 |\Delta U|}{l}} = c_{m1} r_1^2 r_2 + c_{m2} r_1 r_2^2 (r_2 - 0.5) \quad (68)$$

In figure 6 we can the lines for the equations 66, 67, 68 for the case of two real fluids.

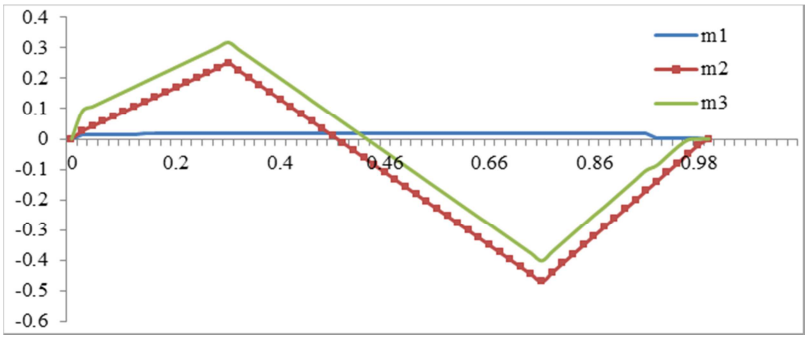

Figure 6. *The rate of transfer mass for m_1, m_2, m_3.*

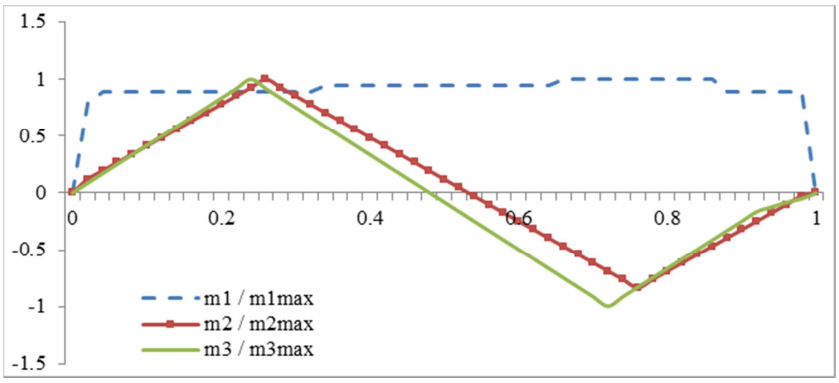

Figure 7. *The rate of transfer mass of m_1, m_2 and m_3.*

We can observe that the modified equation of mass transfer between the two fluids m3 not only describes the entrainment of non-turbulence fluid from the fluid turbulence, but also reveals the rate of mass transfer from the fluid in turbulence non-turbulence fluid. Thus, the rate of mass transfer of the modified equation expresses the proper rate of mass transfer between the two fluids.

14. Results

Figure 8 shows the change of the shear rate near the wall and along axis z. We know that the shear rate is the ratio of shear stress to the local density at each position. It is known that the shear stress (i.e., resistance to flow) is much higher in turbulence flow relative to the laminar flow. This is done as it expresses the continuous exchange of packets of the liquid leaving an area and moved to a different area , traveling at different speeds . This causes either a profit or a loss in momentum so that we have higher or lower values in shear stress. It is reasonable to have higher values at the entrance and the exit, where the flow is more turbulence characteristics with respect to the middle of the container.

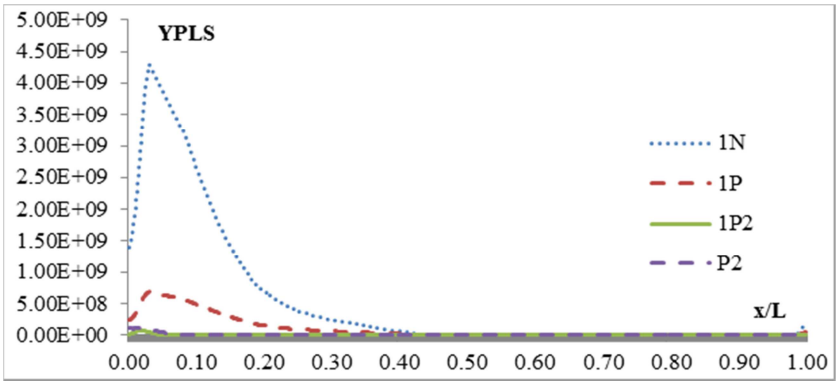

Figure 8. *The shear rate YPLS near the wall and along the tundish length*

As we know the overall viscosity of our fluid given by the sum at each location of the local and the local laminar turbulence viscosity. We have seen that the fluid enters the vessel us in a very short distance, the value of the shear rate ejected gripping the critical value. This is shown in our chart with the top curve that makes us. Finally, we note that it is more strong and abrupt change in the case 1N, and 1P less in very smooth where 1R2 and 2R. In Figure 9 we change the length of the mixing function of the length of our vessel. We see that the mixing length increases from zero to the point where I have complete development of turbulence flow. This increase is more pronounced in the case of single-phase two-stage problem turbulence model k - e than in all other cases.

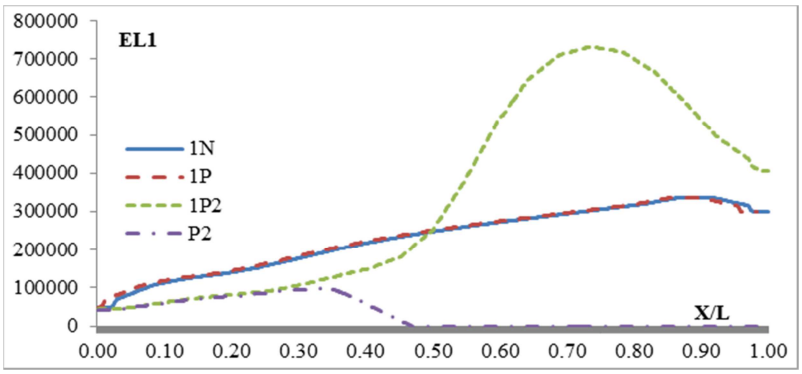

Figure 9. *The mixing length EL1 along the tundish length.*

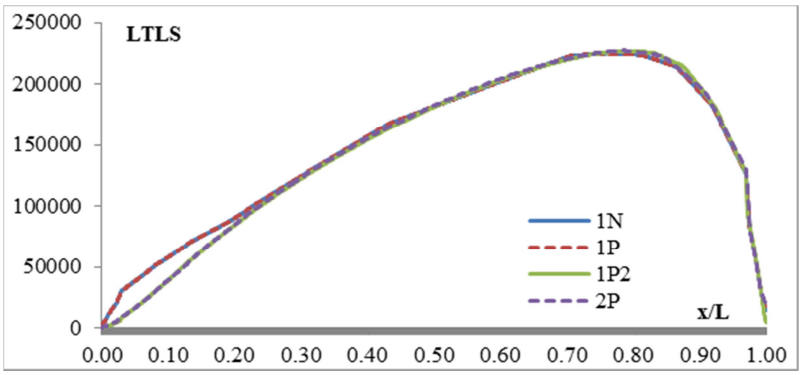

Figure 10. *The change of local scale along the tundish length*

In figure 10 we can see the change of local scale of turbulence along the length of our containers. That our variable has the value:$divgradL = -1$.

The local length scale of the turbulence itself does not express the distance from the wall, but it is part of the link gives me the distance. That actually gives us the change of the distance of each local point P along the vessel us. Thus, if the distance of the point from our y fronts wall of the container and our y1 of the rear wall, we have:

$$y + y_1 = 1 \tag{69}$$

$$L = \frac{y_1 - y}{2} y \tag{70}$$

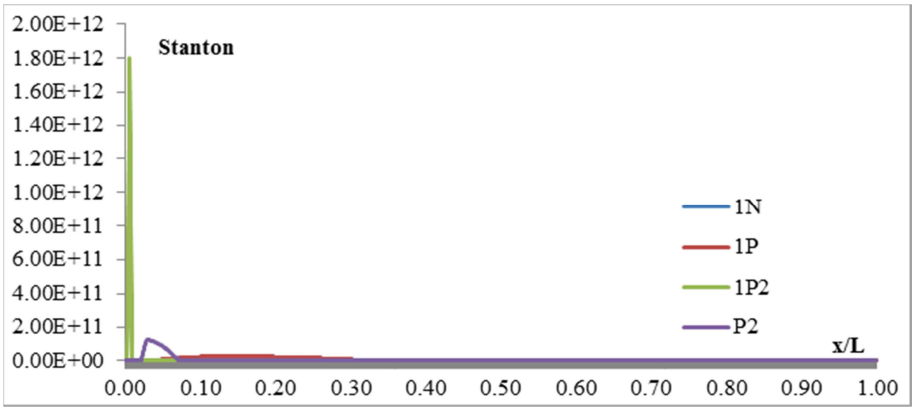

Figure 11. *The Stanton number along the tundish length*

He notes that the rates are similar regardless of the turbulence model and the kind of flow, one fluid or two fluid. In Figure 11 the number Stanton St or CH, expressed along the container us. The Stanton number is a number that measures the ratio of the amount of heat transferred to the fluid to the heat capacity of the fluid you include and characterize the heat transfer in our flow.

$$St = \frac{h}{V\rho C_P} = \frac{Nu}{Re*Pr} \quad (71)$$

The Stanton number arises when considering the geometrical similarity of the dynamics of the boundary layer to the thermal boundary layer, where it can be used to express a relationship between the shear force at the wall (friction) and the total heat transfer to the wall (due thermal diffusion). In figure 12 we can see the change of numbers Reynolds, Stanton along the container.

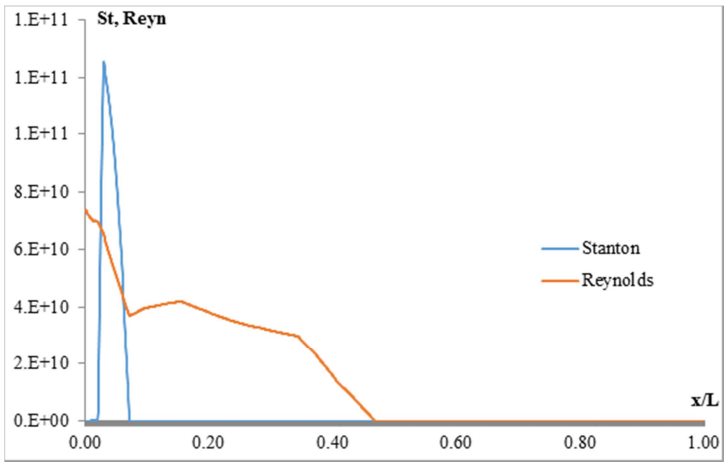

Figure 12. *Compare the Stanton and Reynolds numbers along the tundish length*

In figure 13 we can see the influence of the parameter LC_f along the container for various values when we maintain constant LC_m and C_h.

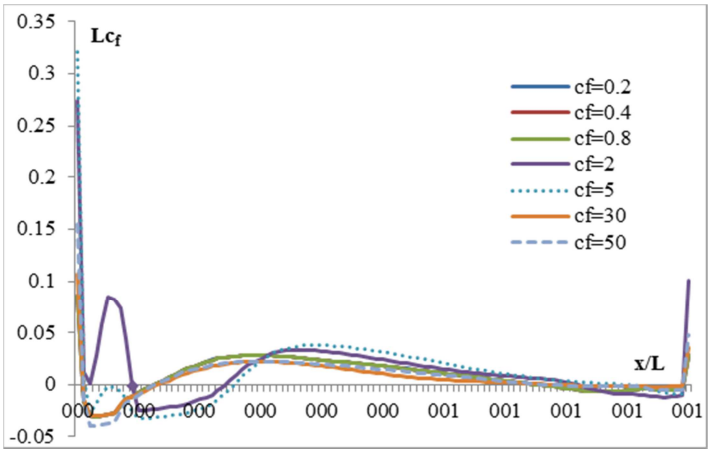

Figure 13. *The LC_f along the tundish length*

Table 9. *Data of LC_f along the tundish length for constant LC_m and C_h.*

L	l_f	C_f	LC_f	K_f	C_m	C_m/C_f
7.50	0.05	0.20	1.50	0.075	10.00	50.00
7.50	0.05	0.40	3.00	0.150	10.00	25.00
7.50	0.05	0.80	6.00	0.300	10.00	12.5
7.50	0.05	2.00	15.00	0.750	10.00	5.00
7.50	0.05	5.00	37.50	1.875	10.00	2.00
7.50	0.05	10.00	75.00	3.75	10.00	1.00
7.50	0.05	30.00	225.00	11.25	10.00	0.333
7.50	0.05	50.00	375.00	18.75	10.00	0.200

Recall that the coefficient LCf referred to as coefficient of resistance (friction parameter). Increasing LC_f causes increased between the two liquid interfaces and lowers the slopes of the properties, etc. From the table 9 we see that for small values of LC_f (1.5-15) no significant difference in results us. The opposite is true for large values of LC_f where for a price of 10 times (37.5 - 375) have multiple corresponding final values (2 - 0.200). Figure 12 shows that with increasing rate LC_f more independently are both fluid and the speed of the first fluid reaches a threshold value. As

shortens the ratio C_m / C_f better mixing occurs and the relative velocity between the two fluids is minimized. In figure 14 we can see the influence of the parameter LC_m along the container for various values when we maintain constant LC_f and C_h.

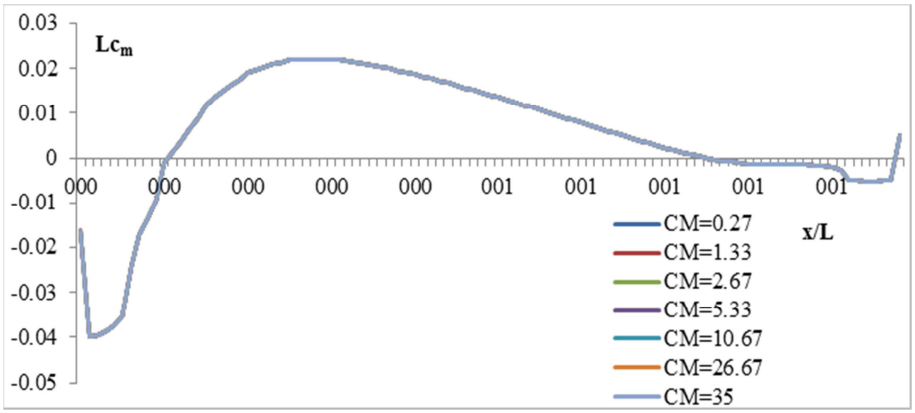

Figure 14. *The LC_m along the tundish length for constant LC_f and C_h*

Table 10. *Data for LC_m along the tundish length for constant LC_f and C_h.*

L	l_f	C_m	LC_m	K_m	C_f	C_m/C_f
7.50	0.05	0.27	2.00	0.10	0.375	0.27
7.50	0.05	1.35	10.00	0.50	0.375	1.35
7.50	0.05	2.70	20.00	1.00	0.375	2.70
7.50	0.05	5.33	40.00	2.00	0.375	5.33
7.50	0.05	10.60	80.00	4.00	0.375	10.70
7.50	0.05	26.70	200.00	10.00	0.375	26.67
7.50	0.05	35.00	262.50	13.125	0.375	35,00
7.50	0.05	40.00	400.00	15.00	0.375	40.00

Recall that the coefficient LC_m referred to as mass transfer coefficient (mass transfer parameter). Increase LC_m causes increased between the two liquid interface and accelerate the integration process.

From Table 10 we see that for large values of LCm (> 100) have almost immediate transfer of mass from the incoming fluid to remain in our container. These values are not interested in this work in accordance with the conditions and restrictions that we have used. Of course, LCm = 300 we have the case of larger and more abrupt mass transfer, which takes place only at the entrance to the container and the nozzle high indeed. In Figure 13 shows the fluid velocity us for various values of LC_m

In figure 15 we can see the difference of the two components of the speed w along the container in various positions x/L. We note that this difference is large at the beginning of our vessel, while dwindling as we go. At this point about 40% of the length of the container, we observe the two components of the equation because we no longer exchange amounts of energy and heat between the two fluids us. Finally, there is a small anomaly at the end of our containers because the fluid exiting through the nozzle.

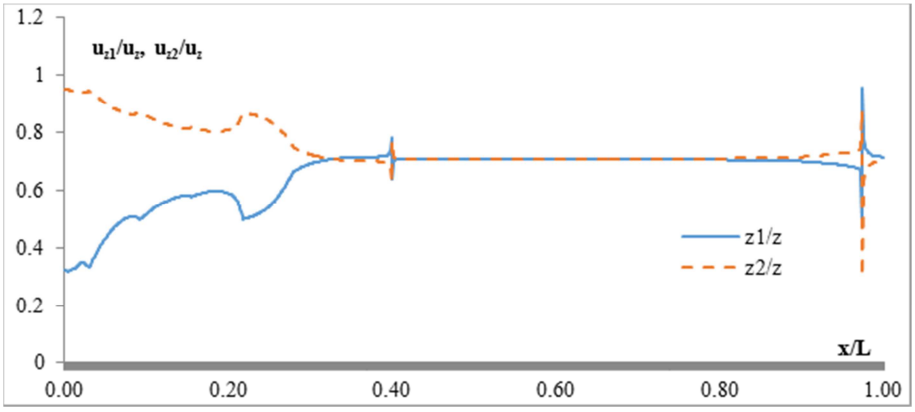

Figure 15. *The difference of the two components of the w speed along the container in various positions x/L*

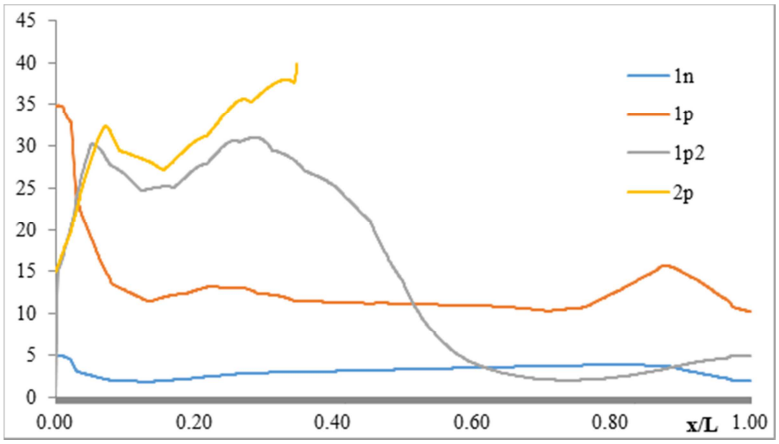

Figure 16. *Predictions of the dissipation rate of turbulence kinetic energy*

The results presented above have shown that the mean flow and temperature characteristics of turbulence shear layers can be reasonably well simulated with the two-fluid model of turbulence. The value of 0.05 obtained for the inter-fluid diffusion heat transfer coefficient is of the same order of magnitude as (but not greater than) that for momentum. It is not surprising that this value differs from that deduced from conditional sampling data. The latter specifically defines the two fluids as turbulence/ non turbulence while the present model distinguishes them by the difference in their cross-stream velocity components. This distinction is reflected through the whole calculation as evident in the comparison of the individual fluid properties with the conditionally-sampled data.

Of special interest is that the same set of constants was used for all predictions which have traditionally required modification of some constants of conventional turbulence models. In addition, predictions of mean flow characteristics including the heat transfer coefficient at the wall appear to be as good as those obtained by other workers with the more popular k-e model. Some of the unacceptable results such as the predicted heat flux in the free shear layers could conceivably be improved upon by adjusting the model constants. However, the effects on the other results would need to be evaluated.

Of course, the large number of constants in the model is a drawback. But since the expressions with which they are associated have physical basis, a set of values such as those in Table 1 that can predict mean flow characteristics reasonably well will probably suffice for practical flow simulation. This work is a small step in the long road to establishing the two-fluid model as a viable tool. A stiffer test demands its application to more complex flow situations including those with significant pressure gradients. This aspect will be the subject of the next investigation.

15. Conclusion

A two-fluid model of turbulence has been used to calculate fluid flow and heat transfer characteristics of turbulence shear layers including flat-plate boundary layer, a plane jet and a round jet. A model is formulated to represent conduction of heat at the interface of the constituent fluids and the associated constant in this model is deduced by reference to available experimental data. The same set of constants is employed for all flows and the model predictions of mean-flow characteristics agree satisfactorily with the experimental data. Further work is being planned to apply the model to more complex flow situations such as those involving significant pressure gradients.

A transient two-fluid model has been developed to simulate fluid flow and heat transfer in a no isothermal water model of a continuous casting tundish. The original liquid in the bath is defined as the first fluid, and the inlet stream, with the temperature variation, is defined as the second fluid. The flow pattern and heat transfer are predicted by solving the three-dimensional transient transport equations of each fluid. The main findings of the numerical investigation are as follows.

When pouring the hotter or cooler water into the water model, the results clearly show the thermal-driven flow pattern, leading to thermal stratification in the bath. The location of the dead zone changed with different thermal conditions.

1. Comparing with the single fluid k-model, the numerical results by using the two-fluid model are in better agreement with the measurements, especially in certain regions and periods. The over evaluation of the conductive heat transfer in the transition region of the system found by using the single fluid with k-model can be eliminated by using the two-fluid model. The two-fluid model can also better describe the counter gradient diffusion phenomenon caused by the thermal buoyancy force.
2. It appears that the two-fluid model may be able to capture the physics of the system better, by considering the interaction of the inlet stream and bulk original liquid. In this study, the temperature difference is the basic index to distinguish the two fluids. Keeping on the same mathematical modeling procedure, the two fluids can also be otherwise defined.
3. When using the k-ε model, relatively high values of the effective viscosity was found throughout, this would

indicate that this model may over predict the diffusive transport of turbulence kinetic energy. An important conclusion of this behavior is that the k-ε model predicts relatively high velocities in a major part of the domain, which seems to be physically consistent with the high values of the effective viscosity. One may suspect that the numerical values of these high velocities maybe quite inaccurate. Nonetheless, the overall picture of a highly turbulence, well mixed region near the inlet and an essentially stagnant or slowly moving laminar region in the remainder of the system appears to be at least qualitatively correct.

4. It appears that the two-fluid model may be able to capture the physics of the system rather better, by considering interaction of a highly turbulence region near the inlet and- an essentially laminar region in the remainder of the system. The preliminary comparison between experimental measurements and the model predictions indicate that this may be quite a promising approach.
5. It should be stressed to the reader, however, that both the k-ε model and the two-fluid model are just "models" of turbulence fluid flow, which rely on certain fundamental postulates and assumptions. A consensus appears to be emerging that the k-ε model has some fundamental flaws, when it comes to representing systems that have both highly turbulence and quiescent portions. The two-fluid model maybe an ideal way to study such situations, without expending a great deal of computational labor. However further work will be needed before such a statement may be made with full confidence.

Nomenclature

C_1	a turbulence coefficient constant
C_2	a turbulence coefficient constant
C_m	a turbulence coefficient constant
F	time-averaged frictional force
g	gravitational acceleration
k	turbulence kinetic energy
K_f	an empirical constant = L/W
K_m	an empirical constant = H/W
P	time-averaged pressure
R	a generic variable
t	time
U	time-averaged velocity
X	Cartesian coordinate
e	turbulence kinetic energy dissipation rate
m	dynamic viscosity
m_e	effective dynamic viscosity
m_t	dynamic eddy viscosity
ρ	substance density
s_k	a turbulence coefficient constant
s_ε	a turbulence coefficient constant
s_Φ	a turbulence coefficient constant
Φ	time-averaged volume fraction

Subscripts

1	first phase
2	second phase
i	component in the *i* direction
k	phase *k*
l	phase *l*
r	ambient fluid
rel	relative value

References

[1] Anestis S. Thesis, 2014. National Technical University of Athens, Greece

[2] Chen C.P., 'Multiple-scale turbulence model in confined swirling- jet predictions', AIAA J., Vol.24, p.1717, (1986).

[3] Fabris G., P.T.Harsha and R.B.Edelman, 'Multiple-scale turbulence modelling of boundary-layer flows for scramjet applications', NASA-CR-3433, 1981.

[4] Hanjalic K. and B.E. Launder, 'Turbulence transport modelling of separating and reattaching shear flows', Mech.Eng.Rept. TF/78/9, University of California, Davis, USA, 1978.

[5] Hanjalic K. B.E. Launder and R. Schiestel. Multiple time scale concept in turbulence transport modeling, 1980, Turbulence Shear flows in Springer Verlag, pp.36-50.

[6] Harlow F. H. and P. I. Nakayama, Turbulence transport equations, Physics FIuia!s lo,2323 (1967).

[7] Ilegbusi O. J. Application of the two-fluid model of turbulence to tundish problems. ISIJ, 1994, vol. 34, 9, pp. 732-738

[8] Ilegbusi O. J. and D. B. Spalding, A two-fluid model of turbulence and its application to near-wall flows, PCH PhysicoChem. Hydrodyn. 9(1/2), 127 (1987).

[9] Ilegbusi O. J. and D. B. Spalding: Int. J. Heat Mass Transf, 32:4 (1989), 767.

[10] Illegbussi O. J. and J. Szekely. Fluid flow and tracer dispersion in shallow tundishes. Steel Res,, vol. 59 (1988), pp.399-405.

[11] Illegbussi O. J. and J. Szekely: Effect of externally imposed magnetic field on tundish performance. Ironmaking Steelmaking, vol.16 (1989), pp. 110-115

[12] Illegbussi O. J. and J. Szekely: Steel Res., 62 (1991), 193.

[13] Jha P.K., Rajeev Ranjan, Swasti S. Mondal and Sukanta K. Dash. Mixing in a tundish and a choice of turbulence model for its prediction. Int. J. Num. Meth. Heat Fluid Flow, vol.13, no 8, 2003, pp 964-996.

[14] Joo S., R.I.L. Guthrie, and C.J. Dobson: Tundish Metallurgy, ISS, Warrendale, PA, 1990, vol. 1, pp. 37-44.

[15] Kim S. W. Near wall turbulence mode; and its application to fully developed turbulence channel and pipe flows. 1990, Numerical Heat Transfer, part B, vol. 17, pp. 101-110

[16] Kim S.W. and C.P.Chen, 'A multi-time-scale turbulence model based on variable partitioning of the turbulence kinetic energy spectrum', Numerical Heat Transfer, Part B, Vol.16, pp193, 1989.

[17] Kim S.W. Calculation of diverged channel flows with a multiple time scale turbulence model. 1991, AIAA J. vol.29, pp.547-554

[18] Launder, B.E. & Spalding, D.B. (1974). The numerical computation of turbulence flows, Computer Methods in Applied Mechanics Engineering, Vol.3, pp. 269–289.

[19] Malin M. R. and D. B. Spalding: PCH Physicochem. Hydrodyn., 1984, vol. 5, p. 339.

[20] Markatos N.C. 1986. The mathematical modeling of turbulence flows. Appl. Math. Modelling, vol.10, pp.190-220

[21] Schiestel R. Multiple scale concept in turbulence modeling II Reynolds stresses and turbulence heat fluxes of a passive scalar, algebraic modeling and simplified model using Boussinesq Hypothesis. J. Mech. Theor. Appl. 1983, vol.2 pp 601-610

[22] Schiestel R. Multiple time scale modeling of turbulence flows in one point closure. Phys. Fluids, 1987, vol. 30, pp. 722-724

[23] Shen, Y.M., Zheng, Y.H., Komatsu, T., Kohashi, N., 2002. A three-dimensional numerical model of hydrodynamics and water quality in Hakata Bay. Ocean Engineering 29 (4), 461–473.

[24] Sheng D.Y. and L. Jonsson: Metall. Trans. B, 1999, pp. 979-85.

[25] Skelland A.H, 1967. 'Non-Newtonian flow and heat transfer', John Wiley, New York, Book Publication.

[26] Spalding D. B., Chemical reaction in turbulence fluids, J. PhysicoChem. Hydrodyn. 4(4), 323 (1982).

[27] Spalding D. B., Towards a two-fluid model of turbulence combustion in gases with special reference to the spark ignition engine, I. Mech. E. Conf., Oxford, April 1983. In Combustion in Engineering, Vol. 1, Paper No. C53/83, pp. 135-142 (1983).

[28] Szekely J., O. J. Ilegbusi and N. EI-Kaddah: PCH Physico Chemical Hydrodynamics, (1987), 9, 3, 453. K. H.

[29] Tacke K.H. and J. C. Ludwig: Steel flow and inclusion separation in continuous casting tundishes. Steel Res. Vol. 58, (1987), pp.262-270.

[30] Lopez-Ramirez S., R.D. Morales, J.A. Romero Serrano, 2000. Numerical simulation of the effects of buoyancy forces and flow control devices on fluid flow and heat transfer phenomena of liquid steel in a tundish. Numerical Heat Transfer, A. vol.37, pp. 37-69.

[31] Anestis Stylianos. The Process of Heat Transfer and Fluid Flow in CFD Problems. American Journal of Science and Technology. Vol. 1, No. 1, 2014B, pp. 36-49